Robust diving control of an AUV

Article *in* Ocean Engineering · January 2009

DOI: 10.1016/j.oceaneng.2008.10.006

CITATIONS
86

READS
1,193

1 author:

Lionel Lapierre
Laboratoire d'Informatique, de Robotique et de Microélectronique de Montpellier (LIRMM)
88 PUBLICATIONS **2,562** CITATIONS

SEE PROFILE

Ocean Engineering 36 (2009) 92–104

Contents lists available at ScienceDirect

Ocean Engineering

journal homepage: www.elsevier.com/locate/oceaneng

Robust diving control of an AUV

Lionel Lapierre *

LIRMM, 161 Rue Ada, 34392 Montpellier, France

ARTICLE INFO

Article history:
Received 7 March 2008
Accepted 23 October 2008
Available online 25 November 2008

Keywords:
Robust control
Nonlinear control
Underwater system
AUV

ABSTRACT

Mobile systems traveling through a complex environment present major difficulties in determining accurate dynamic models. Autonomous underwater vehicle motion in ocean conditions requires investigation of new control solutions that guarantee robustness against external parameter uncertainty. A diving-control design, based on Lyapunov theory and back-stepping techniques, is proposed and verified. Using adaptive and switching schemes, the control system is able to meet the required robustness. The results of the control system are theoretically proven and simulations are developed to demonstrate the performance of the solutions proposed.

1. Introduction

The severe problem of managing water resources leads public and private authorities to finance research of the use of alternative water resources such as karst submarine springs. This is the purpose of the MEDITATE sixth framework program.[1] The Montpellier Laboratory of Computer Science, Robotics, and Microelectronics (LIRMM) is responsible for carrying out physical and chemical water sampling, through the use of its autonomous underwater vehicle (AUV), Taipan 2.

The work reported here focuses on the control of the Taipan 2. Its purpose is to take electrical conductivity and temperature mapping at various depths over a karst water spring. The objective is to obtain sufficient samples to generate an accurate 3D numerical model of the spring in order to quantify its flow and water quality. These measurements must be carried out at different periods of the year in order to evaluate the change in seasonal flow dynamics. This requires accurate geo-referencing of the data. Consequently, the vehicle needs to adjust its trajectory using periodic GPS positioning calibration in an autonomous manner.

An important constraint is the depth at which the springs are located. We are currently performing validation tests on the fresh water spring *La Vise*. The resurgence depth is around 36 m, located at the bottom of an 80-m diameter cone, and rising up to a depth of 2 m.

Initial tests were performed using the Taipan 2. These tests emphasized the necessity for precise control of the vertical trajectory, because the vehicle must be able to navigate in a very shallow environment. The purpose of this paper is to present the design of a robust control law that provides the desired accuracy in the vertical control of an AUV. The performance of the solution is evaluated using simulations.

1.1. Taipan 2: vehicle description

The Taipan 2 AUV is currently being developed by LIRMM (France) and the Hytec/ECA company (France). It is particulary well suited for this type of application because of its small size and weight (1.8 m length, 0.2 m diameter, 60 kg) and relatively low cost. Its design is derived from the torpedo-shaped Taipan 1 AUV. It has a single propeller, a rudder and a stern diving plane. Additional bow diving planes endow the vehicle with new capabilities particularly suited to very shallow water applications. Unlike other similar vehicles (Remus[2], Gavia[3] and Callas[4]), Taipan 2 is able to follow a desired depth profile with a null pitch angle, and dive from the surface autonomously. The bow control planes can counteract the positive buoyancy necessary to guarantee recovery. The Taipan 2 carries a wide range of sensors. For the purpose of navigation the AUV has two depth sensors, the acceleration and orientation unit 3DM-GX1 (Microstrain) and the Workhorse Doppler Velocity Log (RDI Instrument), and it also has a low power GPS Unit (Lassen). The mission specific sensors carried by the vehicle are a side scan sonar (Tritech), a CTD sampler (ADM), a CCD VPC-795DN camera (Pacific Corporation) and two molded underwater transducers (Murata). A third iteration of the vehicle is currently underway, and it will include

* Tel.: +33 4 67 41 85 15; fax: +33 4 67 41 85 00.
E-mail address: lapierre@lirmm.fr

[1] URL: http://www.meditate.hacettepe.edu.tr/prjdesc/sum_just.htm

[2] Hydroin Inc., *Remus homepage*, URL: http://www.hydroidinc.com

[3] Gavia Comp., *Gavia homepage*, URL: http://www.gavia.is/

[4] CNIM., *Callas homepage*, URL: http://www.cnim.fr/

0029-8018/$ - see front matter © 2008 Elsevier Ltd. All rights reserved.
doi:10.1016/j.oceaneng.2008.10.006

an electronic pencil beam sonar (Imagenex) and an acoustic modem (ORCA).

1.2. AUV control

The performance of an AUV controller that is model based depends on the accuracy of the model parameters. Accurate modeling for an AUV is a difficult task, and results in a set of highly coupled nonlinear equations (Aucher, 1981; Fossen, 1994; Lewis, 1988; Batchelor, 1967; Newman, 1977). Controller design resulting from classic linear approaches does not generate satisfactory performances, as exposed by Kim (2000). Silvestre et al. (2002) propose a gain-scheduled trajectory-tracking controller. The linearization of the system dynamics about trimming-trajectory, helices parameterized by the vehicle's linear speed, yaw rate and flight path angle, results in a time-invariant plant. Thus, considering a global trajectory consisting of the piecewise union of trimming trajectories, the problem is thereby solved by designing a set of linear controllers for the linearized plants at each operating point. Interpolating between these controllers guarantees adequate local performance for all the linearized plants. However, this methodology does not explicitly address the issues of global stability and performance.

Accuracy of the model estimation cannot be guaranteed, so the robustness of the control scheme is important. One of the classical control methods relies on the sliding-mode design, exposed by Slotine and Li (1991). Salgado-Jimenez et al. (2004) propose a control design applied to the Taipan 2 AUV, based on a high-order sliding mode, that explicitly addresses the chattering problem encountered when using the classic sliding mode. This is achieved by controlling high-order derivatives of the sliding surface, thus removing the discontinuity of the control vector. This method exhibits robust behavior, but the equivalent control is designed using a linearized method that does not allow for global stability and performance analysis. Song and Smith (2000) combine the sliding-mode advantages with a fuzzy approach expressing the switching rules based on experimental data. This approach allows for the design of a solution without considering any system model. Nevertheless, global stability and performance of this solution still cannot be addressed. Naeem et al. (2002, 2004) propose a control based on model prediction using genetic algorithms, but the performances and stability properties are not addressed. Designing a control scheme that guarantees global convergence requirements is of major interest in the field of autonomous underwater robotics. The final objective is to ensure safe recovery of the vehicle at the end of the mission. This goal requires many different aspects of the system to be simultaneously considered. The hardware and software architectures must exhibit a deterministic behavior. The navigation system should provide a certain estimation of system states within guaranteed error tolerance, and the control scheme must exhibit desirable global performances. Considering the model nonlinearities, the Lyapunov approach has many advantages. A first step allows for designing a control solution that considers the system kinematics and meets global convergence requirements. Then using the backstepping approach (Krstic et al., 1995), the system model is augmented with its dynamic states, while still meeting global performance requirements. Another backstepping stage allows for parameter uncertainty to be taken into account, designing an adaptive scheme that guarantees robustness. This method is only valid if the parameters appear with an affine form in the control expression. An application to a nonholonomic wheeled system has been proposed by Soetanto et al. (2003). In the case of an AUV, the underactuation constraint (where there are fewer actuators than degrees of freedom to be controlled) is expressed at the dynamic level, and its consideration leads to a control expression that contains dynamic parameters which do not appear with an affine form (Lapierre, 2003). Existing solutions are based on a model simplification, reducing the problem to a multivariable linear system (Healey and Lienard, 1993; Fossen, 1994; Prestero, 2001), or using a McLaurin series expansion of the trigonometric terms around a well-chosen guidance function, asJi-Hong and Pan-Mook (2005) did.

Recently, there has been a surge of interest in the problem of coordinated motion control of fleets of autonomous marine vehicles. The work reported in the literature addresses a large class of challenging problems that include, among others, cooperative exploration (Zhang et al., 2007), formation flying (Porfiri et al., 2007; Stilwell and Bishop, 2000) and mobile sensor networks (Ogren et al., 2004) carried by swarms of vehicles.

Our approach considers the vertical dynamic model of the Taipan 2 AUV, taking advantage of the presence of bow control surfaces that yield a control expression where the parameters appear with an affine form. Moreover, the presence of these bow fins makes the system fully actuated in the vertical plane, for nonzero forward velocity. The diving profile can be fully controlled with a desired pitch angle that theoretically can be null. Diving from the surface with a desired null pitch angle might not be efficient. The time to reach the desired depth could become very long. This allows for navigation at the desired depth with a null pitch angle. The positive system buoyancy, necessary for recovery, induces an upward force that must be counteracted by the bow fins. An active buoyant control system could achieve the same goal, but the lack of any controlled organs of this type will result in conflict between the pitch and depth controls.

The paper is organized as follows: Section 2 formulates the problem under study, and presents the kinematic and vertical dynamic models of the Taipan 2 AUV. Section 3 presents the method for designing a dynamic control of the vehicle's depth behavior and introduces the design of the adaptive scheme to achieve the desired robustness. Then another robust scheme is presented, based on switching system theory. Section 4 contains simulation results and discussions. Section 5 concludes the paper.

2. Problem formulation

This section introduces the notation used throughout the paper. The kinematic and vertical dynamic models of the Taipan 2 AUV is presented, and a formulation of the problem of driving a vehicle in the vertical plane is stated.

2.1. Notation

The following notation will be used in the paper. The symbol $\{A\}:=\{x_A, y_A, z_A\}$ denotes a reference frame with origin O_A and unit vectors x_A, y_A and z_A. Given two reference frames $\{A\}$ and $\{B\}$, ${}^B_A R$ is the rotation matrix from $\{B\}$ to $\{A\}$. The general kinematic and dynamic equations of a vehicle can be developed using a global coordinate frame $\{U\}$ and a body-fixed coordinate frame $\{B\}$, as depicted in Fig. 1. Consider the Taipan 2 vehicle with frames and variables defined according to the SNAME convention (SNAME, 1964). Following this convention:

- $[u, v, w]$ defines the linear system velocities (surge, sway and heave, respectively) expressed in the body frame $\{B\}$.
- $[\phi, \theta, \psi]$ defines the vehicle's attitude, designing, respectively, the roll, pitch and yaw angles.
- $[p, q, r]$ denotes the angular velocities about each of the axis of the body coordinate frame. The kinematic relation between $[p, q, r]$ and $[\dot{\phi}, \dot{\theta}, \dot{\psi}]$ is given in Eq. (1).

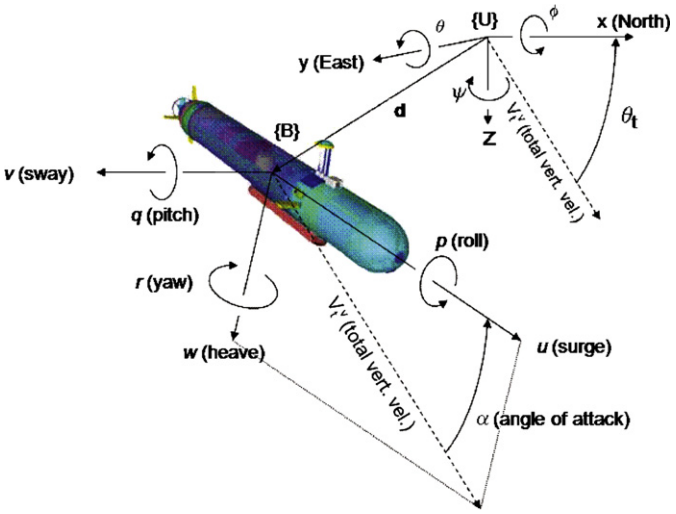

Fig. 1. Body-fixed frame $\{B\}$ and earth-fixed reference frame $\{U\}$.

- v_t^v defines the total velocity projected onto the diving plane, $v_t^v := \sqrt{u^2+w^2}$.
- α is the angle of attack, $\alpha := -\arctan(w/u)$.
- θ_t is the angle of the total velocity vector with respect to the horizontal surface where $\theta_t := \theta + \alpha$.
- δ_r^{up} and δ_r^{up} are the deflection angles of the rudder surfaces. In the Taipan 2, the upper and lower rudder surfaces are independently controlled. This allows compensation of the rolling effect from the thruster.
- δ_b and δ_s are the deflection angle of the bow and stern surfaces, respectively. In the Taipan 2, the portside and starboard surfaces are coupled. Fig. 2 illustrates the definition of the angle of the control surfaces.

Let $d=[x,y,z]$ be the position of $\{B\}$ with respect to $\{U\}$. The complete kinematic model of the AUV is

$$\begin{aligned}
\dot{x} &= u\cos\psi\cos\theta - v\sin\psi\cos\phi + v\cos\psi\sin\theta\sin\phi \\
&\quad + w\sin\psi\sin\phi + w\cos\psi\sin\theta\cos\phi \\
\dot{y} &= u\sin\psi\cos\theta + v\cos\psi\cos\phi + v\sin\psi\sin\theta\sin\phi \\
&\quad - w\cos\psi\sin\phi + w\sin\psi\sin\theta\cos\phi \\
\dot{z} &= -u\sin\theta + v\cos\theta\sin\phi + w\cos\theta\cos\phi \\
\dot{\phi} &= p + q\sin\phi\tan\theta + r\cos\phi\tan\theta \\
\dot{\theta} &= q\cos\phi - r\sin\phi \\
\dot{\psi} &= q\sin\phi/\cos\theta + r\cos\phi/\cos\theta
\end{aligned} \tag{1}$$

The Taipan 2 vehicle dynamic model has been theoretically estimated with the classic methods in Fossen (1994) and Aucher (1981). For control design purpose, and as done in Silvestre et al. (2002), we simplify the full model in neglecting the stable roll motion. Then the simplified vertical plane model can be written as

$$\begin{aligned}
F_u &= m_u\dot{u} + d_u \\
F_w &= m_w\dot{w} + m_{uq}uq + d_w \\
\Gamma_q &= m_q\dot{q} + m_{pr}pr + d_q
\end{aligned} \tag{2}$$

where $m_u = mass - X_{\dot{u}}$, $m_w = mass - Z_{\dot{w}}$, $m_q = I_{yy} - M_{\dot{q}}$, $m_{uq} = -mass$, $m_{pr} = -I_{zz}$, $d_u = -X_{uu}u|u| + mass(qw - vr + z_g(pr))$, $d_w = -Z_{ww}w|w| - Z_{uw}uw - masszg(p^2+q^2)$ and $d_q = -M_{qq}q|q| - M_{uq}uq - M_{uw}uw + (z_g massg - z_b buoyg)\sin\theta + masszg(wq - vr)$.

The variables $X_{..}, Z_{..}$ and $M_{..}$, represent the dynamic derivative coefficients of the vertical plane dynamics of Taipan 2. The terms *mass*, *buoy* and $I_{..}$ are the mass, buoyancy and moments of inertia of the vehicle, respectively. z_g and z_b, respectively, are the location of the center of gravity and the center of buoyancy along the z_B axis with respect to the axis of propulsion. Due to the two planes of symmetry of the vehicle geometry, x_g, y_g and x_b, y_b are zeroes. To simplify, we assume a linear effect for surface deflection. The propulsion model is treated as a constant source and the thrust as it is done by in Prestero (2001). The value of the propulsion coefficients are derived from experiments at sea conducted on Taipan 2. These tests show that the vehicle maintains a forward velocity of $1.5\,\mathrm{m\,s^{-1}}$ with maximum pulse width modulation (PWM) input of the propulsion motor. We assume that at this steady velocity, the system compensates for the axial drag effect. Then the propulsion model coefficients are computed as

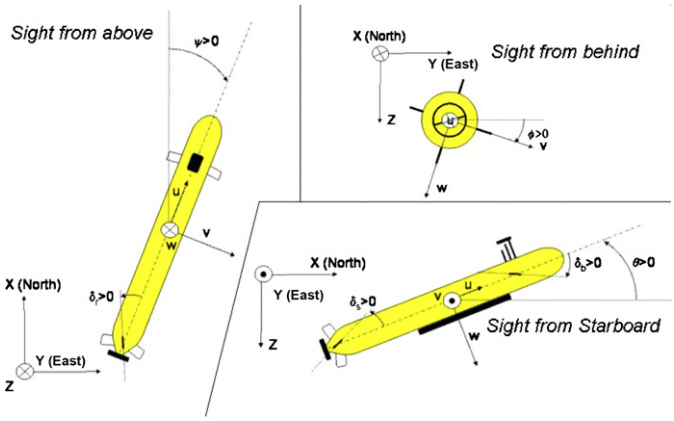

Fig. 2. Body frame and control surfaces angles definition.

$$X_{uprop} = -X_{uu}(1.5)^2 \tag{3}$$

Taking into account these assumptions, the vertical plane actuation model can be written as follows:

$$\begin{aligned}
F_u &= X_{uprop} \\
F_w &= Z_{uu\delta_b}u^2\delta_b + Z_{uu\delta_s}u^2\delta_s \\
\Gamma_q &= M_{uu\delta_b}u^2\delta_b + M_{uu\delta_s}u^2\delta_s
\end{aligned}$$

Table 1 (see Appendix A) gives the dimensional values of these derivatives for Taipan 2.

2.2. Problem formulation

Our objective is to design a control law for the system described by its kinematic and dynamic models (1) and (2) to asymptotically reach a desired depth profile, regardless of misestimation in model parameters, and assuming negligible roll dynamics. The design process will include three steps. We will first consider the kinematic level, and proceed to a Lyapunov-based control design that exhibits asymptotic global performances. The second step consists of augmenting the considered system with its dynamic states (2), and using backstepping techniques, design a dynamic control that respects the previous convergence requirement. The third stage will again use a backstepping process to explicitly consider the effect of parameter misestimation on the global performance, and design a robust control scheme to remove this effect. Here we propose two different methods. First we establish the robust scheme design using classic Lyapunov theory. Then we use switching-system theory to achieve the same goal. The previous problems are mathematically stated as follows:

Kinematic problem C_1. *Consider the AUV kinematic equations given by* (1)*, traveling with a forward velocity u. Given a desired depth z_d, derive a feedback control law for the w and q velocities so*

that the depth error $\tilde{z} = z - z_d$ and the pitch angle θ tend uniformly and asymptotically to zero.

The solution to problem C_1 allows for designing kinematic references for the velocities w and q in order to drive the depth z to desired depth z_d and the pitch angle θ to 0. Then this solution is used during a backstepping process to compute the force and torque inputs, in terms of F_w and Γ_q, in order to follow the previous kinematic references. This is the topic of the dynamic problem C_2.

Dynamic problem C_2. *Consider the AUV kinematic and dynamic equations given by* (1) and (2), *propelled with the parameters of Eq.* (3). *Given a desired depth z_d, derive a feedback control law for the bow (δ_b) and stern (δ_s) fins so that the depth error $\tilde{z} = z - z_d$ and the pitch angle θ tend uniformly and asymptotically to zero.*

The previous solution assumes an impossibly perfect knowledge of the system parameters. Problem C_3 includes in its statement the misestimation of the system parameters, and the solution exposed in the sequel proposes the design of a classic adaptive scheme. That allows for the convergence requirement despite parameters misestimation.

Adaptive dynamic problem C_3. *Consider the AUV kinematic and dynamic equations given by* (1) *and* (2), *propelled with the parameters of Eq.* (3). *Given a set of estimated parameters $\hat{X}_{\cdot}$, $\hat{Z}_{\cdot}$, $\hat{M}_{\cdot}$, $\hat{I}_{\cdot}$, $\hat{z}_g$, $\hat{z}_b$, $\hat{mass}$ and $\hat{buoy}$ and a desired depth z_d, derive a feedback control law for the bow (δ_b) and stern (δ_s) fins so that the depth error $\tilde{z} = z - z_d$ and the pitch angle θ tend uniformly and asymptotically to zero.*

As shown in Section 4.3, the previous adaptive solution does not guarantee the existence of a bound in the evolution of the value of the system parameters used in the control expression. Therefore, this solution is not well suited for practical applications. Problem C_4 proposes another statement, that requires two sets of parameters values. The first set is guaranteed to overestimate the real parameters value, and the second is guaranteed to underestimate the real parameters value. Section 4.4 proposes the design of a switching control that guarantees the convergence of the system, despite misestimation of the parameters, while guaranteeing the constraints on the control inputs. This is the switching robust problem C_4.

Switching robust problem C_4. *Consider the AUV kinematic and dynamic equations given by* (1) and (2), *propelled with the parameters of Eq.* (3). *Given a set of estimated parameters, that are guaranteed to overestimate their respective real values $\overline{X}_{\cdot}$, $\overline{Z}_{\cdot}$, $\overline{M}_{\cdot}$, $\overline{I}_{\cdot}$, $\overline{z}_g$, $\overline{z}_b$, $\overline{mass}$ and $\overline{buoy}$, a set of underestimated parameters $\underline{X}_{\cdot}$, $\underline{Z}_{\cdot}$, $\underline{M}_{\cdot}$, $\underline{I}_{\cdot}$, $\underline{z}_g$, $\underline{z}_b$, $\underline{mass}$ and $\underline{buoy}$ and a desired depth z_d, derive a feedback control law for the bow (δ_b) and stern (δ_s) fins so that the depth error $\tilde{z} = z - z_d$ and the pitch angle θ tend uniformly and asymptotically to zero.*

The next section proposes a solution to problems $\mathbf{C_i}$, $i = 1, \ldots, 4$.

3. Control design

This section proposes a solution to the problems stated in the previous section. The complexity of the problem is generally reduced by using an appropriate guidance strategy. This is a method to shape the expression of the error function that the control law tries to reduce to zero. Many guidance strategies have been proposed, see Naeem (2002) for a review. An interesting study case, where a guidance strategy solves the problem of relaxing the classic path-following constraint in the horizontal plane applied to a nonholonomic wheeled or underactuated marine robots, is treated by Soetanto et al. (2003) and Lapierre et al. (2003). Here we consider a nonlinear guidance strategy inspired by the work of Samson and Ait-Abderrahim (1991).

Previous work (Lapierre et al., 2003) addressed the problem of path-following control of an underactuated AUV in the horizontal plane. One of the conclusions was that controlling total velocity horizontal direction (through the control of yaw dynamics), according to an appropriate guidance function, allows for asymptotically and uniformly driving of the origin of the body-frame attached to the vehicle onto the desired path. Due to the unactuated sway dynamics, the results show that the vehicle is driven onto the path, but that the heading is not permanently tangent to the path. This can also be seen in the case of a straight-line path with a lateral sea current. The analogy with our present application (in the diving plane) is straightforward. Consider an AUV that only carries stern control-surfaces. The presence of positive buoyancy plays a similar role to the sea current in the previous horizontal path-following application. Thus, a depth control using only the stern planes will result in a system that naturally compensates for buoyancy by pitching negatively. The use of the bow-plane control will enable counteracting of this ascending effect, thus controlling the pitch dynamics.

Regarding the proofs of the following propositions, we will extensively use a corollary of Barbalat's Lemma and LaSalle's Theorem, stated as follows:

Barbalat's Lemma. *If $f(t)$ is a double differentiable function such that $f(t)$ is finite as t goes to ∞, and such that $\dot{f}(t)$ is uniformly continuous, then $\dot{f}(t)$ tends to* 0 *as t tends to ∞*

Uniform continuity sufficient condition. *$\dot{f}(t)$ is uniformly continuous if $\ddot{f}(t)$ exists and is bounded.*

Corollary of Barbalat's Lemma (CBL). *If $f(t)$ is a double differentiable function such that $f(t)$ is finite as t goes to ∞, and such that $\ddot{f}(t)$ exists and is bounded, then $\dot{f}(t)$ tends to* 0 *as t tends to ∞.*

LaSalle's invariance principle. *Let Ω be a positively invariant set of the autonomous system described in* (1) and (2). *Suppose that every solution starting in Ω converges to a set $E \subset \Omega$ and let M be the largest invariant set contained in E. Then every bounded solution starting in Ω converges to M as t tends to ∞.*

See Slotine and Li (1991) for details on Barbalat's Lemma and its application. For the proof and application of LaSalle's Theorem, see Sepulchre et al. (1997) and Khalil (2002). Note that the application of LaSalle's Theorem is restricted to autonomous systems. However, since in our situation the references of the system (known forward velocity u, desired depth z_d, desired null pitch angle) are known and constant, and the system parameters are constant we fall in this category and we can apply LaSalle's invariance principle.

Regarding Proposition 4, we omit the complete proof. The solution relies on switching system theory and a rigorous proof should introduce some notion about the switching capability of the system (minimum dwell time), that is dependant on the onboard hardware and software architectures. In order to avoid complications, we restrict ourself to simply sketch a proof.

3.1. Kinematic control design

The following proposition suggests a solution to problem $\mathbf{C_1}$.

Proposition 1. *Consider the AUV kinematic equations given by* (1), *traveling with a forward velocity u. Let z_d be the desired depth the vehicle has to reach with a null pitch angle. Let λ and λ_t be two*

guidance functions described by the following equations:

$$\lambda = \lambda^A \tanh(k^A \tilde{z}) \tag{4}$$

$$\lambda_t = \lambda_t^A \tanh(k_t^A \tilde{z}) \tag{5}$$

where k^A, k_t^A *are positive gains,* $0<\lambda^A<\pi/2$ *and* $0<\lambda_t^A<\pi/2$ *are the positive maximum values of the guidance references* λ *and* λ_t *and* $\tilde{z} = z - z_d$ *is the depth error. The following velocity profile, described by Eqs.* (6) *and* (7)*, for q and w, solves problem* $\mathbf{C_1}$.

$$q = \frac{\dot{\theta}^{REF} + r\sin\phi}{\cos\phi} \tag{6}$$

$$w = \int_0^t \left[(\dot{\lambda}_t - \dot{\theta}^{REF} - k_w(\theta_t - \lambda_t)) \frac{(v_t^v)^2}{u} \right] dt \tag{7}$$

where $\dot{\theta}^{REF} = [\dot{\lambda} - k_\theta(\theta - \lambda)]$ *and* k_θ, k_w *are positive gains.*

Proof of Proposition 1. Consider the Lyapunov candidate $V_1 = \frac{1}{2}(\theta - \lambda)^2 + \frac{1}{2}(\theta_t - \lambda_t)^2$. Straightforward computation shows that

$$\begin{aligned} \dot{\theta} &= \dot{\lambda} - k_\theta(\theta - \lambda) \\ \dot{\alpha} &= \dot{\lambda}_t - \dot{\theta} - k_w(\theta_t - \lambda_t) \end{aligned} \tag{8}$$

yields $\dot{V}_1 = -k_\theta(\theta - \lambda)^2 - k_w(\theta_t - \lambda_t)^2 \leqslant 0$. Since V_1 is a positive and monotonically decreasing function, $\lim_{t\to\infty} V_1(t)$ exists. It is straightforward to show that $\ddot{V}_1$ exists and is bounded. Then, an application of Barbalat's Lemma allows for the conclusion that $\lim_{t\to\infty} \dot{V}_1(t) = 0$. Hence the related variables θ and θ_t are bounded, and asymptotically converge to the invariant set Ω_1 defined as $\Omega_1 := \{(\theta, \theta_t) \in \Re^2 / \theta = \lambda, \theta_t = \lambda_t\}$. Let us now study the system trajectory onto the set Ω_1, considering the Lyapunov candidate function $V_2 = \frac{1}{2}\tilde{z}^2$, defined onto the invariant set Ω_1. Tedious but straightforward algebraic computation shows

$$\dot{V}_2 = u\tilde{z}\left[-\sin\lambda\left(1 - \frac{\cos\phi}{1 + \tan\lambda\tan\lambda_t}\right) - \frac{\tan\lambda_t\cos\lambda}{1 + \tan\lambda\tan\lambda_t}\cos\phi + \frac{v}{u}\cos\theta\sin\phi \right]$$

The previous expression is composed with three terms, in which appear the rolling angle ϕ and the side slip angle $\beta = \arctan(v/u)$. Clearly these terms are dependent on the horizontal and the rolling-plane controllers. Studying the coupling between the three planes could be an interesting question, but will lead in this work to unnecessary complications. So, as mentioned in the problem statement, we neglect the roll effect dynamics. The previous expression thus becomes

$$\dot{V}_2 = u\tilde{z}\left[\frac{-\tan\lambda_t}{1 + \tan\lambda\tan\lambda_t} \frac{1}{\cos\lambda} \right]$$

Considering the definition of the guidance functions (4) and (5), we know that $-\pi/2<\lambda<\pi/2$, $-\pi/2<\lambda_t<\pi/2$ and that both functions have the same sign than $\tilde{z}$. Then we conclude that $\dot{V}_2(t) \leqslant 0$ onto Ω_1 and for all t. Since V_2 is positive and monotonically decreasing, $\lim_{t\to\infty} V_2(t)$ exists, hence $\tilde{z}$ is bounded. Since $\tilde{z}$ is bounded, $\dot{V}_2$ and $\dot{\tilde{z}}$ are also bounded. Then, direct derivation shows that the condition of boundedness for $\ddot{V}_2$ is met. The application of Barbalat's Lemma onto the invariant set Ω_1 allows for the conclusion that $\lim_{t\to\infty} \dot{V}_2(t)|_{\Omega_1} = 0$. So $\lim_{t\to\infty} \tilde{z}(t)|_{\Omega_1} = 0$. Hence, considering the definition of λ, we conclude that $\lim_{t\to\infty} \theta(t) = 0$ onto Ω_1. Consequently, the set defined by $(\tilde{z} = 0, \theta = 0)$ is the unique invariant set of Ω_1. We conclude that the control described in (8) ensures that every system trajectory converges to the set where $(\tilde{z} = 0, \theta = 0)$. A simple manipulation of the kinematic equations shows that Eqs. (6) and (7) realize control (8). □

Expression (7) might appear complex for a kinematic control. In fact, designing a kinematic control for a dynamic system such an AUV does not make much sense. As we have already noted (Lapierre et al., 2003), the kinematic design injects dynamics into the process. This is why the control expression (7) contains an integral. As we will see in the sequel, the design of the dynamic control is much simpler, but relies on the previously stated results.

3.2. Dynamic control design

The next proposition suggests a solution to problem $\mathbf{C_2}$.

Proposition 2. *Consider the AUV kinematic and dynamic equations given by* (1) *and* (2)*, propelled with the parameters of Eq.* (3)*. Let* z_d *be the desired depth the vehicle has to reach with a null pitch angle and* λ *and* λ_t *the two guidance functions defined by Eqs.* (4) *and* (5)*, where* k^A, k_t^A *are positive gains,* $0<\lambda^A<\pi/2, 0<\lambda_t^A<\pi/2$ *are the positive maximum values of the guided variables and* $\tilde{z} = z - z_d$ *is the depth error. The dynamic control is then defined as follows*:

$$\begin{bmatrix} \delta_b \\ \delta_s \end{bmatrix} = A^{-1} \begin{bmatrix} F_w^{CONT} \\ \Gamma_q^{CONT} \end{bmatrix} \tag{9}$$

where

$$A = u^2 \begin{bmatrix} Z_{uu\delta_b} & Z_{uu\delta_s} \\ M_{uu\delta_b} & M_{uu\delta_s} \end{bmatrix} \tag{10}$$

and

$$\begin{aligned} F_w^{CONT} &= m_w \dot{w}^{CONT} + m_{uq} uq + d_w \\ \Gamma_q^{CONT} &= m_q \dot{q}^{CONT} + m_{pq} pq + d_q \end{aligned} \tag{11}$$

where

$$\begin{aligned} \dot{w}^{CONT} &= \frac{-(v_t^v)^2 \dot{\alpha}^{REF} + w(X_{prop} - d_u)/m_u}{u} \\ \dot{q}^{CONT} &= \dot{q}^{REF} - k_q(q - q^{REF}) \end{aligned} \tag{12}$$

and

$$\begin{aligned} \dot{\alpha}^{REF} &= \dot{\lambda}_t - \dot{\theta}^{REF} - k_w(\theta_t - \lambda_t) \\ q^{REF} &= \frac{\left(\dot{\theta}^{REF} + r\sin\phi\right)}{\cos\phi} \\ \dot{\theta}^{REF} &= \dot{\lambda} - k_\theta(\theta - \lambda) \end{aligned} \tag{13}$$

where k_θ, k_q *and* k_w *are positive gains that solves problem* $\mathbf{C_2}$.

Proof of Proposition 2. Consider the expressions of Eq. (8) as a reference to drive the dynamic AUV model. These references are also reported in (13). Consider the Lyapunov candidate $V_3 = \frac{1}{2}(q - q^{REF})^2 + \frac{1}{2}(\theta_t - \lambda_t)^2$. Clearly the choice of the acceleration profile:

$$\begin{aligned} \dot{q} &= \dot{q}^{REF} - k_q(q - q^{REF}) \\ \dot{\alpha} &= \dot{\lambda}_t - \dot{\theta} - k_w(\theta_t - \lambda_t) \end{aligned}$$

yields $\dot{V}_3(t) = -k_q(q - q^{REF})^2 - k_w(\theta_t - \lambda_t)^2 \leqslant 0$, for all t. Considering the dynamic model (2), the application of the force and torque expressed in (11) realize the previous acceleration profile. One step further consists in taking into account the (simple) actuation model and results in the expression of the fin control in (9). Since V_3 is a positive, monotonically decreasing function, $\lim_{t\to\infty} V_3(t)$ exists. Showing that $\ddot{V}_3$ is bounded is trivial, and an application of Barbalat's Lemma allows for stating that $\lim_{t\to\infty} \dot{V}_3 = 0$. Then, the system trajectories asymptotically converge to an invariant set Ω_2 defined as $\Omega_2 := \{(q, \theta_t) \in \Re^2 / q = q^{REF}, \theta_t = \lambda_t\}$. Let us now study the system trajectories onto the Ω_2 set. Since $q|_{\Omega_2} = q^{REF}$,

$\dot{\theta}|_{\Omega_2} = \dot{\lambda} - k_\theta(\theta - \lambda)$. The consideration Lyapunov candidate $V_4 = \frac{1}{2}(\theta - \lambda)^2$ onto the Ω_2 set allows for the conclusion that the evolution of θ is asymptotically and uniformly converging to an invariant subset of Ω_2, that is Ω_1 itself. Considering the system convergence properties onto the set Ω_1 stated in the previous proof, the application of LaSalle's Theorem allows for the conclusion that $\tilde{z}$ and θ are asymptotically and uniformly converging to zero. □

Expression (9) drives the dynamic model of the AUV to a desired depth, controlling the pitch angle with the guidance function λ. This control expression implies a perfect knowledge of the system parameters which is impossible to reach. The next section proposes the design of an adaptive scheme that preserves the asymptotic and uniform convergence requirement, despite parameter misestimation.

3.3. Robust adaptive control design

The following proposition suggests a solution to problem $\mathbf{C_3}$.

Proposition 3. *Consider the AUV kinematic and dynamic equations given by* (1) and (2), *propelled with the parameters of Eq.* (3). *Let* $\hat{X}_{\cdot\cdot}$, $\hat{Z}_{\cdot\cdot}$, $\hat{M}_{\cdot\cdot}$, $\hat{I}_{\cdot\cdot}$, $\hat{z}_g$, $\hat{z}_b$, $\hat{mass}$ *and* $\hat{buoy}$ *be a set of estimated parameters. And let* z_d *be the desired depth the system has to reach with a null pitch angle. Then, the following control expression solves problem* $\mathbf{C_3}$.

$$\begin{bmatrix} \delta_b \\ \delta_s \end{bmatrix} = A^{-1} \begin{bmatrix} F_w^{CONT} \\ \Gamma_q^{CONT} \end{bmatrix}$$

where A is expressed in Eq. (10), *and*

$$\Gamma_q^{CONT} = \sum_{i=1}^{7} f_i p_i$$

$$F_w^{CONT} = \sum_{j=1}^{8} g_j q_j \tag{14}$$

with

$$\begin{aligned} &g_1 = \dot{w}^{CONT}, \quad f_1 = \dot{q}^{CONT} \\ &g_2 = \cos\theta\cos\phi, \quad f_2 = -uw \\ &g_3 = vp, \quad f_3 = pr \\ &g_4 = -uq, \quad f_4 = wq - vr \\ &g_5 = -(p^2 + q^2), \quad f_5 = \sin\theta \\ &g_6 = w|w|, \quad f_6 = q|q| \\ &g_7 = uw, \quad f_7 = uq \\ &g_8 = uq \end{aligned} \tag{15}$$

and

$$\begin{aligned} &\dot{p}_i = -k_i^p(q - q^{REF})f_i, \quad i = 1,\ldots,7 \\ &\dot{q}_j = -k_j^q(\theta_t - \lambda_t)\frac{u}{(v_t^v)^2}g_j, \quad j = 1,\ldots,8 \end{aligned} \tag{16}$$

considering the following parameter initial value:

$$\begin{aligned} &q_1^0 = \hat{mass} - \hat{Z}_{\dot{w}}, \quad p_1^0 = \hat{I}_{yy} - \hat{M}_{\dot{q}} \\ &q_2^0 = -(\hat{mass} - \hat{buoy})g, \quad p_2^0 = \hat{M}_{uw} \\ &q_3^0 = \hat{mass}, \quad p_3^0 = \hat{I}_{zz} \\ &q_4^0 = \hat{mass}, \quad p_4^0 = \hat{z}_g\hat{mass} \\ &q_5^0 = \hat{z}_g\hat{mass}, \quad p_5^0 = (\hat{z}_g\hat{mass} - \hat{z}_b\hat{buoy})g \\ &q_6^0 = -\hat{Z}_{ww}, \quad p_6^0 = -\hat{M}_{qq} \\ &q_7^0 = -\hat{Z}_{uw}, \quad p_7^0 = -\hat{M}_{uq} \\ &q_8^0 = -\hat{Z}_{uq} \end{aligned} \tag{17}$$

where k_θ, k_q, k_w, k_i^p *and* $k^q{}_j$, *with* $i = 1,\ldots,7$ *and* $j = 1,\ldots,8$, *are positive gains. The expression of* $\dot{q}^{CONT}$ *and* $\dot{w}^{CONT}$ *can be obtained from Eq.* (12).

Note that the parameter adaptation does not concern the actuation model. Considering the simplicity of the considered actuation model, the adaptation of its parameters is not significant. To avoid coupling expressions of the controlled torque and force, we have decided to remove the fin parameters from the adaptation scheme. Note that the distribution of signs between p_i and f_i and between q_j and g_i has been carried out in order to guarantee the positiveness of parameters p_i and q_i.

Proof of Proposition 3. Consider the expressions of the controlled force and torque in (11). These expressions are rewritten using in (14). The functions g_j and f_i are written in (15). The values of parameters p_i and q_j can be found in (17). Note that the two expressions (11) and (14) are equivalent if the parameters q_j and p_i are constant and computed with the real dynamic parameter values of Table 1 (see Appendix A). Let us call this optimal evaluation p_i^{opt} and q_j^{opt} and note that these values are positive (cf. the comment at the end of the statement of Proposition 3). Consider now that the evaluation of parameters q_j and p_i is made with estimated values of the Taipan 2 parameters. Let $\tilde{p}_i = p_i - p_i^{opt}$ and $\tilde{q}_j = q_j - q_j^{opt}$ be the estimation errors. The application of $\Gamma_q^{opt} = \sum_{i=1}^{7} p_i^{opt} f_i$ and $F_w^{opt} = \sum_{j=1}^{8} q_i^{opt} g_i$ guarantees the asymptotic convergence of the system, as seen previously. But, the application of $\Gamma_q^{CONT} = \sum_{i=1}^{7} p_i f_i$ and $F_w^{CONT} = \sum_{j=1}^{8} q_i g_i$ induces a nonnegative $\dot{V}_3$ Lyapunov derivative:

$$\begin{aligned} \dot{V}_3 = &-k_q(q - q^{REF})^2 + (q - q^{REF})\left(\sum_{i=1}^{7}\frac{\tilde{p}_i f_i}{p_i^{opt}}\right) \\ &-k_w(\theta_t - \lambda_t)^2 + (\theta_t - \lambda_t)\left(\sum_{j=1}^{8}\frac{\tilde{q}_j g_j}{g_j^{opt}}\frac{u}{(v_t^v)^2}\right) \end{aligned} \tag{18}$$

Let V_5 be another Lyapunov candidate.

$$V_5 = V_3 + \frac{1}{2}\left[\sum_{i=1}^{7}\frac{1}{k_i^p}\frac{(\tilde{p}_i)^2}{p_i^{opt}} + \sum_{j=1}^{8}\frac{1}{k_j^q}\frac{(\tilde{q}_j)^2}{q_j^{opt}}\right] \tag{19}$$

Note that p_i^{opt} and q_j^{opt} are constant and positive, hence V_5 is positive definite, $\dot{\tilde{p}}_i = \dot{p}_i$ and $\dot{\tilde{q}}_i = \dot{q}_i$. Then, the adaptation scheme (16) yields $\dot{V}_5 = \dot{V}_3 \leqslant 0$. The convergence proof follows the same idea as that used in the previous proof. □

The definition of p_i, f_i, q_j and g_j guarantee the positivity of the parameters p_i and q_j. It is necessary to ensure that the Lyapunov function V_5 is positive definite. This requires a previous knowledge of the parameters' signs. This is generally the case, but not always. Moreover, as simulation results will show, the previous solution analysis is incomplete. Indeed, nothing in the considered Lyapunov function prevents the parameter adaptation evolution to diverge despite the fact that the global convergence is mathematically guaranteed.

The next solution proposes a robust control design based on switching-system theory that does not require adaptation.

3.4. Robust switching control design

The following proposition suggests a solution to problem $\mathbf{C_4}$.

Proposition 4. *Consider the AUV kinematic and dynamic equations given by* (1) and (2), *propelled with the parameters of Eq.* (3). *Consider a set of estimated parameters, guaranteed to overestimate their respective real value* $\overline{X}_{\cdot\cdot}$, $\overline{Z}_{\cdot\cdot}$, $\overline{M}_{\cdot\cdot}$, $\overline{I}_{\cdot\cdot}$, $\overline{z}_g$, $\overline{z}_b$, $\overline{mass}$ *and* $\overline{buoy}$, *and set of underestimated parameters* $\underline{X}_{\cdot\cdot}$, $\underline{Z}_{\cdot\cdot}$, $\underline{M}_{\cdot\cdot}$, $\underline{I}_{\cdot\cdot}$, $\underline{z}_g$, $\underline{z}_b$, $\underline{mass}$ *and* $\underline{buoy}$. *Let* z_d *be the desired depth the system has to reach with a null pitch*

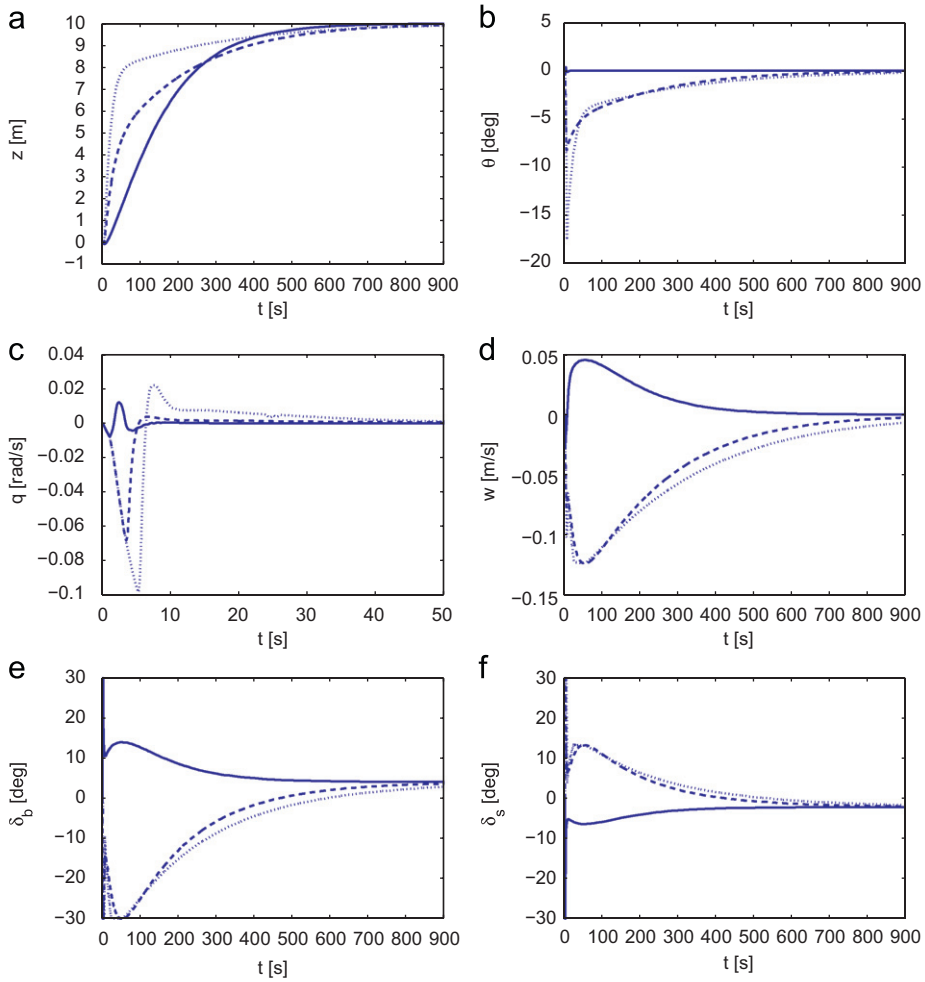

Fig. 3. Simulations results of the dynamic control, when considering a perfect knowledge of the parameters. (a) Depth evolution. (b) Pitch angle evolution. (c) Pitch velocity evolution. (d) Heave velocity evolution. (e) Bow plane evolution. (f) Stern plane evolution.

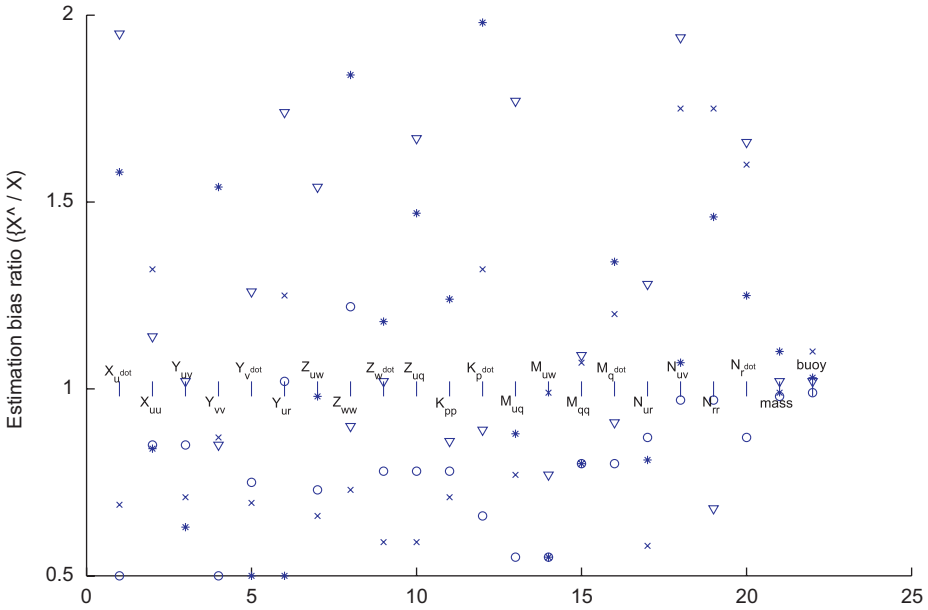

Fig. 4. The estimation bias for the four sets of parameters.

angle. Then, the following control scheme solves problem $\mathbf{C_4}$:

$$\begin{bmatrix}\delta_b\\ \delta_s\end{bmatrix} = A^{-1}\begin{bmatrix}F_w^{CONT}\\ \Gamma_q^{CONT}\end{bmatrix}$$

where A is expressed in Eq. (10), *and*

$$\Gamma_q^{CONT} = \sum_{i=1}^{7} f_i p_i$$
$$F_w^{CONT} = \sum_{j=1}^{8} g_j q_j \qquad (20)$$

where the functions f_i *and* g_j *are defined in* (15). *Parameters* $\overline{p}_i$, $\overline{g}_j$ *and* $\underline{p}_i$, $\underline{g}_j$ *are computed with their respective overestimated and underestimated parameters, in order to ensure that* $\tilde{p}_i = \overline{p}_i - p_i^{opt} > 0$, $\tilde{q}_j = \overline{q}_j - q_j^{opt} > 0$, $\tilde{p}_i = \underline{p}_i - p_i^{opt} < 0$ *and* $\tilde{q}_j = \underline{q}_j - q_j^{opt} < 0$. *And consider the following switching scheme:*

$$\textbf{if } (q - q^{REF})f_i \geqslant 0 \quad \textbf{then } p_i = \underline{p}_i \textbf{ else } p_i = \overline{p}_i, \quad i = 1,\ldots,7$$
$$\textbf{if } (\theta_t - \lambda_t)g_j \geqslant 0 \quad \textbf{then } q_j = \underline{q}_j \textbf{ else } q_j = \overline{q}_j, \quad j = 1,\ldots,8 \qquad (21)$$

Sketch of proof for Proposition 4. Consider the Lyapunov derivative function $\dot{V}_3$ of Eq. (18). A possible solution to ensure the negativity of this function is to choose the sign of $\tilde{p}_i$ and $\tilde{q}_j$. The switching scheme (21) plays this role. But this time the proof cannot rely on Barbalat's Lemma, because of the discontinuity of the control signal (we cannot prove that $\ddot{V}_3$ is bounded). The proof is based on the switching system theory exposed in Hespanha et al. (1999) and Liberzon (2001). It is based on a geometrical analysis of the convergence of the discontinuous Lyapunov candidate, V_3 in our case. V_3 consists in a piecewise union of uniform and asymptotically convergent Lyapunov functions. Each function contributes to the convergence of the system. The problematic point is the impact of the switching on the global convergence property: the switch should not imply a jump in the evolution of the function that affects the convergence. In our situation, since $V_3(t_{sw}^-) = V_3(t_{sw}^+)$, where t_{sw} is the instant when the switching occurs, the global convergence criterion is respected. But a situation where an infinite switching occurs, for example around the zeros of the switching conditions $(q - q^{REF})f_i$ and $(\theta_t - \lambda_t)g_j$, must be taken into account. Since there is no system able to follow this kind of behavior, convergence toward the origin cannot be guaranteed. One way to tackle this problem could be to consider the maximum switching delay (dwell time) necessary for the system, and evaluate the worst possible system reaction during this period. This would allow the definition a zone around the desired references that the system is guaranteed to reach. However the overlapping convergence of the different references would have to be proved. This warrants further research.

The next section presents simulation results to illustrate the performances of the proposed solutions.

4. Simulation results

A C++ simulator based on the Taipan 2 dynamic model (cf. Table 1) has been developed. We present in the sequel simulation results to illustrate the performances of the proposed control law. We are assuming that the sensors provides an estimation of the states of the system with a period of 100 ms. Measurement noise is not considered in the theoretical framework. Nevertheless, some simulations include noisy measurements to illustrate the limits of the proposed methods. We consider that the rolling dynamics are compensated by a static stabilization (i.e. a differential offset of the rudder planes: $\delta_r^u p = 0.06$ and $\delta_r^u p = -0.06$ rad). The desired depth is set to $z_d = 10.0$ m.

During the simulations, the fin amplitude has been limited to $\pm 30^\circ$ to mimic the behavior of Taipan 2. The simulation results can be found in Appendix A. The performances displayed in these figures have to be qualitatively considered.

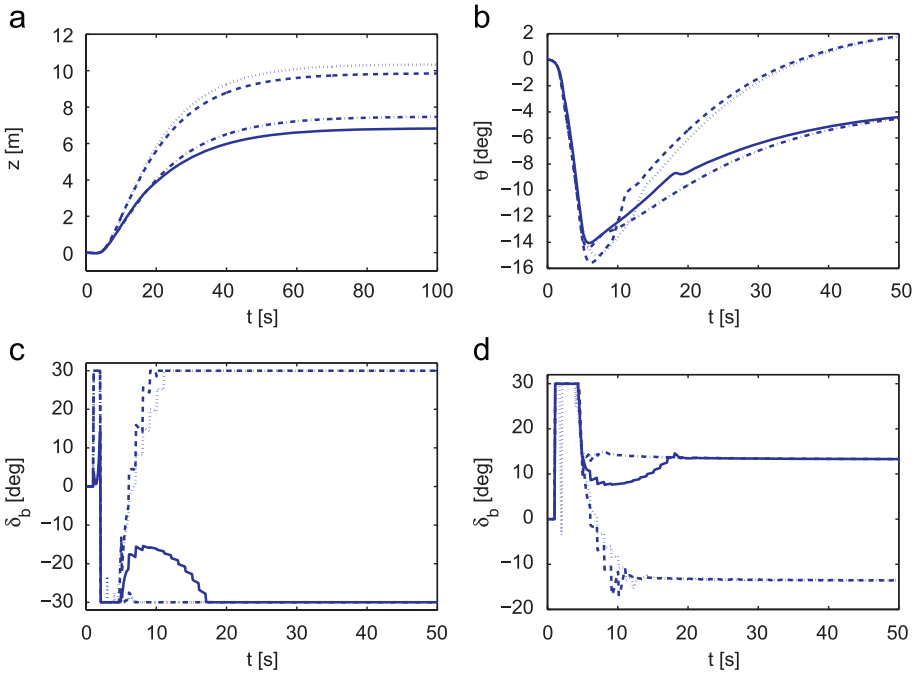

Fig. 5. Simulation results of the dynamic control, using four misestimated sets of parameters. (a) Depth evolution. (b) Pitch angle evolution. (c) Bow plane evolution. (d) Stern plane evolution.

4.1. Dynamic controller

The equations related to Proposition 3 have been implemented in the simulator. Recall that this solution assumes a perfect knowledge of the dynamic parameters. The control gains and parameters used for this simulation are given in Table 2. The simulations results are displayed in Figs. 3a–f, reported in Appendix A.

These simulations were carried out considering three different λ guidance functions. As expected, the convergence rate depends on the guidance amplitude λ^A (cf. Figs. 3a and b). The evolution of w (Fig. 3d) and q (Fig. 3c) velocities clearly shows the stabilization of the system at the desired reference. Figs. 3e and f indicate the difference of strategy in the evolution of the control surfaces. In the case where diving with a constant null pitch is required (solid lines) the bow and stern control surfaces are positioned in a different direction than that resulting of the nonnull pitch control (dashed and dotted lines). Recall that these results have been obtained by supposing a perfect knowledge of the system parameters.

To illustrate the performances of the following robust controllers, we carried out simulations considering four different sets of misestimated parameters. These parameters were randomly estimated using the matlab function $\hat{X} = X + 2 * X * (rand - 0.5)$ for the positive estimation bias, and $\hat{X} = X + X * (rand - 0.5)$ for the negative estimation bias, where X represents

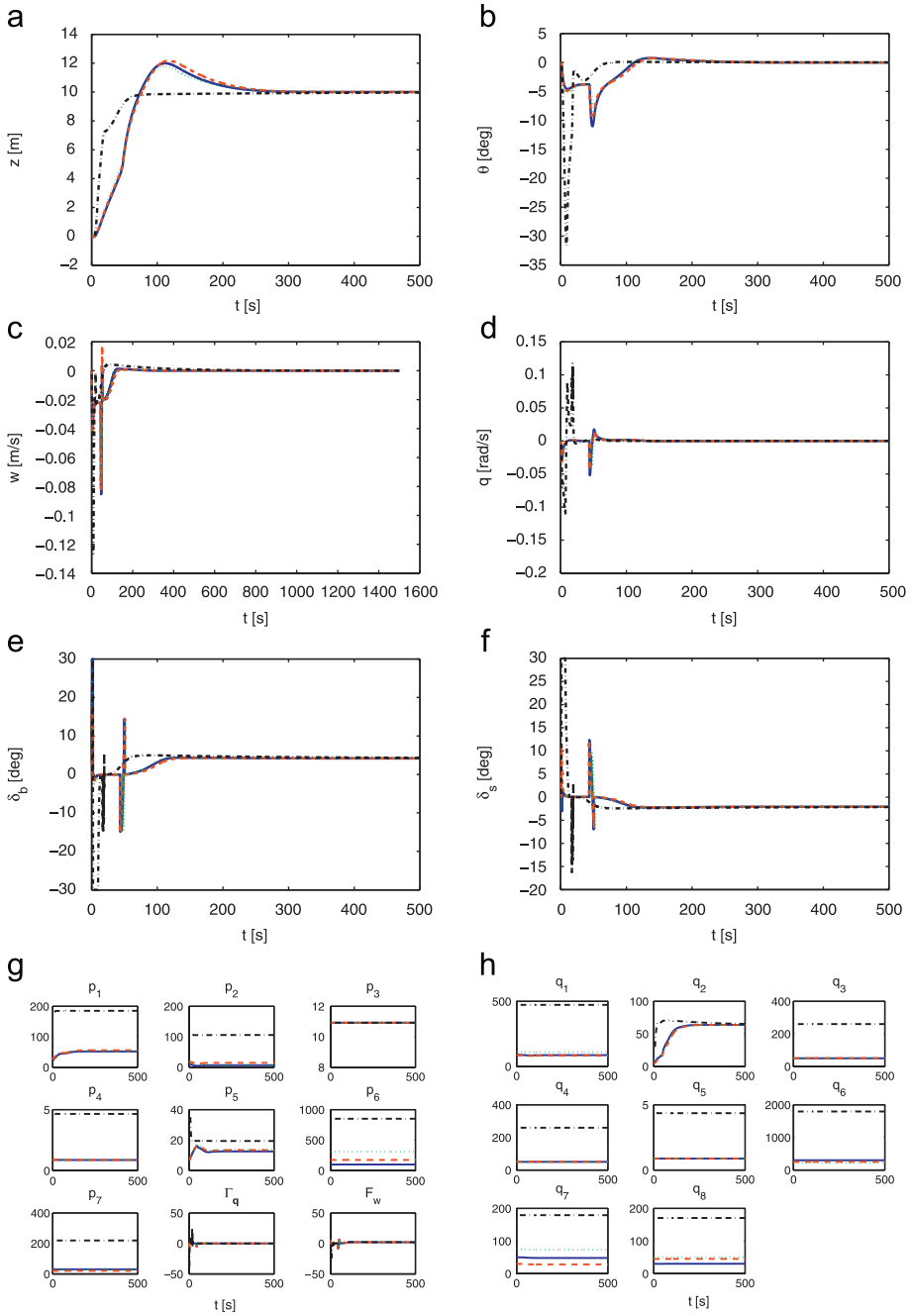

Fig. 6. Simulation results of the adaptive dynamic control, using four misestimated sets of parameters. (a) Depth evolution. (b) Pitch angle evolution. (c) Heave velocity evolution. (d) Pitch velocity evolution. (e) Bow plane evolution. (f) Stern plane evolution. (g) Parameters p_i adaptation evolution. (h) Parameters q_j adaptation evolution.

the real parameter value. This results in a reasonable estimation error, where the estimated parameters are included between twice and half the real parameter value. Some of the parameters (mass, buoy, moments of inertia) can be estimated with a high degree of accuracy. A smaller estimation deviation has been applied to these. The parameter estimation bias is displayed in Fig. 4.

Figs. 5a–d (displayed in Appendix A) show the convergence problem created by this misestimation. In this case, the system cannot clearly achieve the convergence. Another phenomenon must be considered. The effect of saturation on the fins makes the system converge to a local minimum. This problem will not be explicitly studied in this paper. But, as we will see in the sequel, the adaptive or robust switching scheme avoids this problem.

4.2. Adaptive controller

We have implemented the adaptive controller solution using the four sets of misestimated parameters. The adaptation gains have been chosen according to $k_i^p = k_j^q = 20$, $i = 1,\ldots,7, j = 1,\ldots,8$. The results are displayed in Figs. 6a–h, reported in Appendix A. These results show similar performances for the four sets of parameters. Effectively, Figs. 6e and f indicate the same control plane evolution regardless of the initial value of the estimated parameters. Studying the results of the evolution of the parameter adaptation in Figs. 6g and h shows that, as expected, the parameter estimations do not converge to their respective real values. This is a known behavior of this type of adaptive Lyapunov-based controller. Indeed, the Lyapunov function derivative $\dot{V}_5 = \frac{1}{2}(q - q^{REF})^2 + \frac{1}{2}(\theta_t - \lambda_t)^2$ does not contain any term related to the evolution of the parameter-adaptation to any static value. Nevertheless, Figs. 6g and h show the parameter convergence. This convergence is achieved for $q - q^{REF} = 0$ and $\theta_t - \lambda_t = 0$, that is, when guidance error is null.

To illustrate the efficiency and the limitations of this controller, we proceed to another simulation without considering any parameter value. The initial value of the parameter groups appearing in controllers p_i and q_j were set to 1. This is equivalent to consider the system without any parameter estimation. Moreover, the desired depth reference has been chosen as $z_d = 10$, 20,

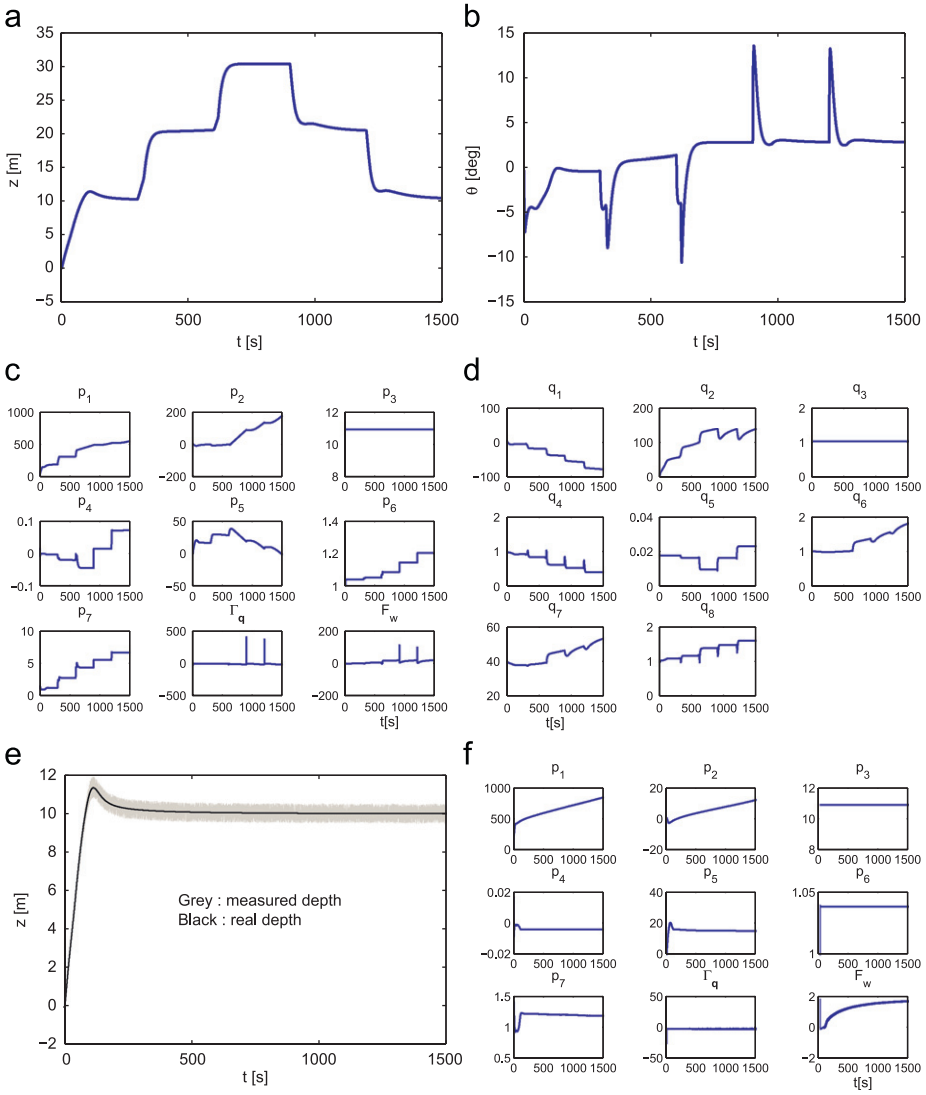

Fig. 7. Simulation results of the adaptive control, showing an unbounded behavior of the parameters adaptation, with a nonautonomous reference z_d (a–d) and with measurement noise (e and f). (a) Depth evolution. (b) Pitch angle evolution. (c) Parameters p_i adaptation evolution. (d) Parameters q_j adaptation evolution. (e) Depth evolution. (f) Evolution of parameters p_i.

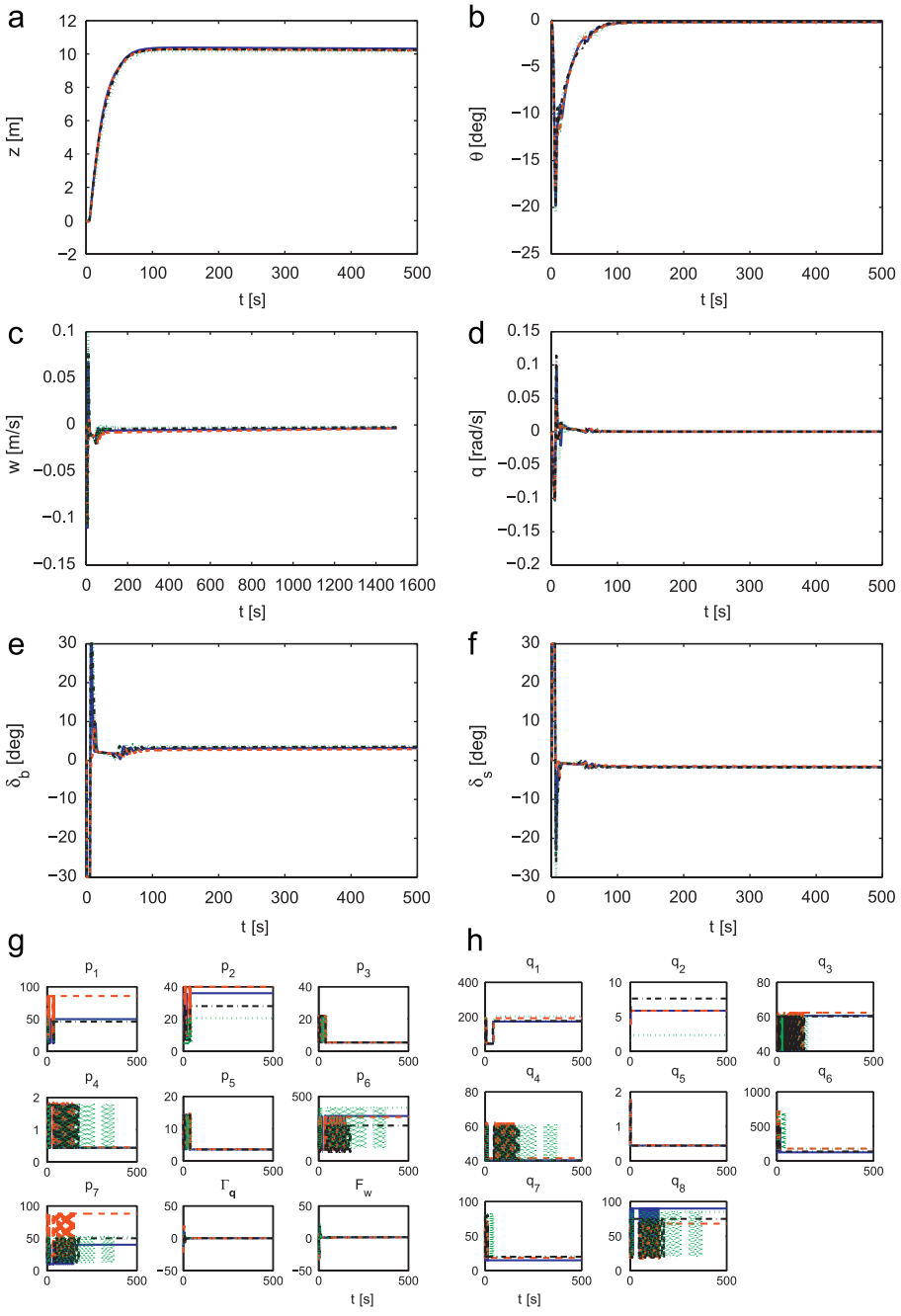

Fig. 8. Simulation results of the switching control. (a) Depth evolution. (b) Pitch angle evolution. (c) Heave velocity evolution. (d) Pitch velocity evolution. (e) Bow plane evolution. (f) Stern plane evolution. (g) Parameters p_i adaptation evolution. (h) Parameters q_j adaptation evolution.

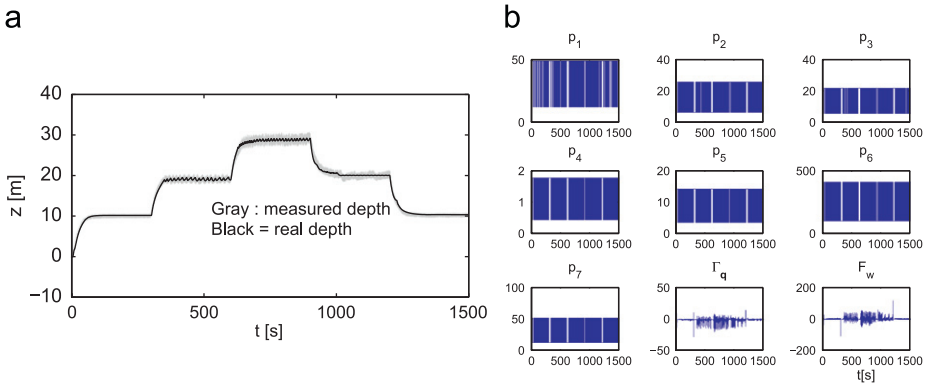

Fig. 9. Simulation results of the switching control, in presence of the measurement noise and using a nonautonomous reference z_d. (a) Depth evolution. (b) Evolution of parameters q_j.

30, 20 and 10 m. This choice was made to focus on the main drawback of this method, which is, nothing prevents the adaptation evolution of the parameters reaching an unbounded value, which is problematic since this parameter value is required in the control computation. The results are displayed in Appendix A.

The results of Figs. 7a and b display good system behavior, despite the initial unitary parameter value. Nevertheless, adaptation evolution of the parameters in Figs. 7c and d indicates an unbounded evolution of parameters p_1, p_2 and q_2. The cause of this can be found in the expression of the adaptation scheme of parameter $\dot{p}_1$. Clearly, this expression includes a term of the form $k_p^1 k_q (q - q^{REF})^2$. That is, the presence of an error in the guidance following will result in a monotonic increase in the p_1 parameter value. In order to demonstrate this undesired behavior in the presence of measurement noise, we carried out a test using noisy measurements of z and θ, with a desired depth $z_d = 10$ m. Figs. 7e and f, displayed in Appendix A, illustrate this behavior. While the system is converging to the desired depth, the value of parameter p_1 is constantly increasing.

From the analysis of the expression of the Lyapunov function V_5 we can deduce that there is no guarantee for the parameters evolution to be bounded. Moreover, under these conditions, the effect of measurement noise could also lead to some unbounded behavior. Another choice for this Lyapunov function may solve this problem.

The next section illustrates the performances of a switching-based robust control that avoids this drawback.

4.3. Robust switching controller

To validate the performances of this controller, we considered the four previous sets of estimated parameters. We doubled the value of each to produce the overestimated set, and halved the value to obtain the underestimated set. An exception concerns parameters q_2, q_3 and q_4, for which the upper value was produced by multiplying the estimated value by 1.2, and by 0.8 for the lower value. This is justified by the fact that the related values *mass* and *buoy* can be accurately estimated. Moreover, from the control point of view, doubling (or halving) these parameters induces a huge and undesired system reaction. The results are reported in Appendix A.

Figs. 8a and b show a good system reaction, clearly converging to the references. Nevertheless, results show a small static error. This error must be compared with the simulation results in Figs. 5a and b, to evaluate the improvement. It is caused by noncentered estimation bias, and is a function of the system dwell time. The theoretical evaluation of this static error could be an interesting study.

Velocity stabilization is shown in Figs. 8c and d. Fin action is displayed in Figs. 8e and f. The switching evolution of the parameter values are displayed in Figs. 8g and h.

Finally, in order to show that the drawbacks of the previous solution are avoided, we carried out a simulation with measurement noise, and considered a varying depth reference $z_d = 10$, 20, 30, 20 and 10 m. These results are not provided to prove any performances related to measurement-noise rejection, but simply to show that the presence of such noise does not lead to system instability. Fig. 9a, reported in Appendix A, shows the system converging toward the reference, with the expected chattering behavior. This kind of behavior could be reduced by filtering the orders sent to the controlled surfaces, or by using the same strategy as that employed in high-order sliding-mode control. Note in Fig. 9b that the presence of measurement noise implies a maximum switching rate (theoretically infinite) of the parameter values. In this situation an explicit study of the dwell-time effect could allow the quantification of system performances. Note the similarity of this switching solution to the sliding-mode approach. In both solutions, the switching effect is used to obtain robustness. The study of this analogy will be an interesting subject for further research.

5. Conclusion

The goal of this paper is to accurately control the depth of an AUV in the presence of parametric modeling uncertainty. First a dynamic diving controller was used, assuming a perfect knowledge of the dynamic parameters. Then, an adaptive scheme was designed to obtain the desired robustness. Simulations extended the theoretical results and led to consider a unitary initial parameter value. In this situation, the desired convergence is achieved despite the large parameter misestimation. Moreover, internal stability problems concerning parameter evolution have been identified and analyzed. Indeed, the presence of measurement noise induces a monotonic drift in the evolution of some parameters. This undesired behavior prevents the implementation of this solution to a real system. Therefore, we proposed another robust scheme based on switching-system theory. We have shown that this switching-control method is implementable and preserves robustness.

Appendix A

A.1. The coefficients of the Taipan 2 vertical plane dynamic model

The hydrodynamic coefficients of the Taipan 2 AUV is presented in Table 1.

The control parameters used for the dynamic control simulation are presented in Table 2.

Table 1
The hydrodynamic dimensional coefficients of the Taipan 2 AUV.

Dimensioned hydrodynamic vertical plane coefficients of the Taipan 2 AUV		
X	Z	M
$X_{uu} = -4.00\,\mathrm{kg\,m^{-1}}$	$Z_{uw} = -40.750\,\mathrm{kg\,m^{-1}}$	$M_{uq} = -34.192\,\mathrm{kg\,m\,rad^{-1}}$
$X_{\dot{u}} = -5.070\,\mathrm{kg}$		
	$Z_{ww} = -350.00\,\mathrm{kg\,m^{-1}}$	$M_{uw} = 10.280\,\mathrm{kg}$
	$Z_{\dot{w}} = -50.700\,\mathrm{kg}$	
	$Z_{uq} = -37.327\,\mathrm{kg\,rad^{-1}}$	$M_{qq} = -200.00\,\mathrm{kg\,m^2\,rad^{-2}}$
		$M_{\dot{q}} = -18.020\,\mathrm{kg\,m^2\,rad^{-1}}$
	$Z_{uu\delta_b} = 4.4913\,\mathrm{kg\,m^{-1}\,rad^{-1}}$	$M_{uu\delta_b} = -8.4729\,\mathrm{kg\,rad^{-1}}$
	$Z_{uu\delta_s} = -4.4913\,\mathrm{kg\,m^{-1}\,rad^{-1}}$	$M_{uu\delta_s} = -16.874\,\mathrm{kg\,rad^{-1}}$
$z_g = 0.01757\,\mathrm{m}$	$mass = 50.7\,\mathrm{kg}$	$I_{yy} = 10.900\,\mathrm{kg\,m^2}$
$z_b = 0.00316\,\mathrm{m}$	$buoy = 50.9\,\mathrm{kg}$	$g = 9.81\,\mathrm{m\,s^{-2}}$

Table 2
The control parameters used for the dynamic control simulation.

Parameter values of the dynamic control simulation		
$k_\theta = 1$ $k_q = 1$ solid line (deg.)	$k_w = 1$ $k^A = 0.1$ dashed line (deg.)	$k_t^A = 0.1$ $z_d = 10$ m. dotted line (deg.)
$\lambda^A = 0.0$	$\lambda^A = -10.0$	$\lambda^A = -20.0$
$\lambda_t^A = -2.0$	$\lambda_t^A = -2.0$	$\lambda_t^A = -2.0$

References

Aucher M., 1981. Dynamique des sous-marins. Internal Report of the Science et technique de l'armemement institution.

Batchelor, G., 1967. An Introduction to Fluid Dynamics, first ed. Cambridge University Press, Cambridge.

Fossen, T., 1994. Guidance and Control of Ocean Vehicles. Wiley, NY, USA.

Healey, A., Lienard, D., 1993. Multivariable sliding mode control for autonomous diving and steering of unmanned underwater vehicles. IEEE Journal of Oceanic Engineering 18 (3), 327–339.

Hespanha, J., Liberzon, D., Morse, A., 1999. Logic based switching control of a non-holonomic system with parametric modeling uncertainties. System and Control Letters, Special Issue on Hybrid Systems 38 (3), 167–177.

Ji-Hong, L., Pan-Mook, L., 2005. Design of an adaptive nonlinear controller for depth control of an autonomous underwater vehicle. Oceanic Engineering 32, 2165–2181.

Khalil, H., 2002. Nonlinear Systems. Prentice-Hall, Upper Saddle River, NJ, USA.

Kim, M., 2000. Nonlinear control and robust observer design for marine vehicles. Ph.D Dissertation, Virginia Polytechnic Institute and State University, Blacksburg, Virginia, USA, November 3.

Krstic, M., Kanellakopoulos, I., Kokotovic, P., 1995. Nonlinear and Adaptive Control Design. Wiley, NY, USA.

Lapierre, L., Soetanto, D., Pascoal, A., 2003. Non-linear path-following control of an AUV. In: Proceedings of the Guidance and Control of Underwater Vehicle (GCUV) Conference, Newport, South Wales, UK, April.

Lewis, E., 1988. Principles of naval architecure. In: Vol. I: Stability and Strength, 1988. Vol. II: Resistance, Propulsion and Vibration, 1988. Vol. III: Motions in Waves and Controllability, 1989. Edition of the Society of Naval Architects and Marine Engineers (SNAME), New York, USA.

Liberzon, D., 2001. Control using logic and switching, part 1: switching in systems and control. In: Handout notes. CDC'01 Workshop, September 4–7. URL: ⟨http://black.csl.uiuc.edu/~liberzon/⟩.

Naeem, W., 2002. Model predictive control of an autonomous underwater vehicle. In: Proceedings of UKACC 2002 Postgraduate Symposium, Sheffield, UK, September, pp. 19–23.

Naeem, W., Sutton R., Ahmad S., Burns R., 2002. A review of guidance laws applicable to unmanned underwater vehicles. In: Reports of the Marine and Industrial Dynamic Analysis Group. URL: ⟨www.cranfield.ac.uk/sims/marine/research/guidance.pdf⟩.

Naeem, W., Sutton, R., Ahmad, S., 2004. Pure pursuit guidance and model predictive control of an autonomous underwater vehicle for cable/pipeline tracking. IMarEST Journal of Marine Science and Environment, Part C (1) 15–25.

Newman, J., 1977. Marine Hydrodynamics, first ed. MIT Press, Cambridge.

Ogren, P., Fiorelli, E., Leonard, N., 2004. Cooperative control of mobile sensor networks: adaptive gradient climbing in a distributed environment. IEEE Transactions on Automatic Control 49 (8), 1292–1302.

Porfiri, M., Gray Roberson, D., Stilwell, D., 2007. Tracking and formation control of multiple autonomous agents: a two-level consensus approach. IFAC Journal Automatica 43 (8), 1318–1328.

Prestero, T., 2001. Verification of a six degree of freedom simulation model for the REMUS autonomous underwater vehicle. Master Thesis in Mechanical Engineering, MIT.

Salgado-Jimenez, T., Spiewak, J.M., Fraisse, P., Jouvencel, B., 2004. A robust control algorithm for AUV: based on a high order sliding mode. In: Proceedings of the MTS/IEEE International Conference, OCEANS'04, Kobe, Japan, November 9–12, 2004, pp. 276–281.

Samson, C., Ait-Abderrahim, K., 1991. Mobile robot control part 1: feedback control of a nonholonomic mobile robot. Technical Report No. 1281, INRIA, Sophia Antipollis, France, June.

Sepulchre, R., Jankovic, M., Kokotovic, P., 1997. Contructive Nonlinear Control. Springer, Berlin.

Silvestre, C., Pascoal, A., Kaminer, I., 2002. On the design of gain-scheduled trajectory tracking controllers. International Journal of Robust and Nonlinear Control 12, 797–839.

Slotine, J., Li, W., 1991. Applied Nonlinear Control. Prentice-Hall, NJ, USA.

SNAME, 1964. Nomenclature for treating the motion of a submerged body through a fluid. Technical and Research Bulletin nos. 1–5 of the Society of Naval Architects and Marine Engineers, New York, USA.

Soetanto, D., Lapierre, L., Pascoal, A., 2003. Adaptive, non-singular path following control of a wheeled robot. In: Proceedings of the IEEE Conference on Decision and Control (CDC), Maui, Hawaii, USA, December.

Song, F., Smith, S., 2000. Design of sliding mode fuzzy controllers for an autonomous underwater vehicle without system model. In: Proceedings of the MTS/IEEE Conference OCEANS'2000 MTS/IEEE, pp. 835–840.

Stilwell, D., Bishop, B., 2000. Platoons of underwater vehicles. IEEE Control Systems Magazine 20 (6), 45–52.

Zhang, F., Fratantoni, D., Paley, D., Lund, J., Leonard, E., 2007. Control of coordinated patterns for ocean sampling. International Journal of Control 80 (7), 1186–1199.